PHYSICAL REVIEW A VOLUME 38, NUMBER 8 OCTOBER 15, 1988

Mode-conversion process and overdense-plasma heating in the electron cyclotron range of frequencies

S. Nakajima and H. Abe
Department of Electronics, Kyoto University, Kyoto 606, Japan
(Received 6 July 1988)

Through a particle-simulation investigation, a new mode-conversion process, through which an incident fast extraordinary mode (fast X mode) is converted into an electron Bernstein mode (B mode) via a slow extraordinary mode (slow X mode), is discovered in plasmas whose maximum density exceeds the cutoff density of the slow X mode. The converted B mode is found to heat the electrons efficiently in an overdense plasma region, when the plasma has the optimum density gradient at the plasma surface.

The mode-conversion processes of the electron-cyclotron-range frequency wave (ECRW) have been studied extensively.[1-9] These processes are expected to play the crucial role in electron cyclotron heating of overdense plasmas, whose maximum density exceeds the cutoff densities of both the ordinary mode (O mode) and the X mode. In the case of O-mode injection into overdense plasmas, several theoretical investigations have been performed.[1-3] For X-mode injection, two mode-conversion processes, the fast X to the B mode and the slow X to the B mode, have been investigated only in low-density plasmas.[4-9] There have been no publications on the mode-conversion processes of the X mode in high-density plasmas, which include the cutoff of the slow X mode. In this paper we report the existence of a new mode-conversion process, referred to as the FX-SX-B process, in such high-density plasmas. Further, we show the theory of this process and give particle simulation results which show a comparison between the theory and the measurement of the absorption coefficient, and indicate good overdense-plasma heating.

Figure 1 shows the refractive indices $N_\perp(=ck_\perp/\omega_0)$ of the X mode and the B mode calculated from the linear dispersion relation, where ω_{pe} and Ω_e are the electron plasma and cyclotron frequencies, respectively, and ω_{UH} is the upper hybrid resonance (UHR) frequency ($\omega_{UH}^2=\omega_{pe}^2+\Omega_e^2$). Here, the cutoffs of the fast and the slow X modes are denoted as $\omega_0=\omega_R$ and $\omega_0=\omega_L$, where ω_R and ω_L are the cutoff frequencies of right- and left-handed elliptic-polarized waves, respectively.

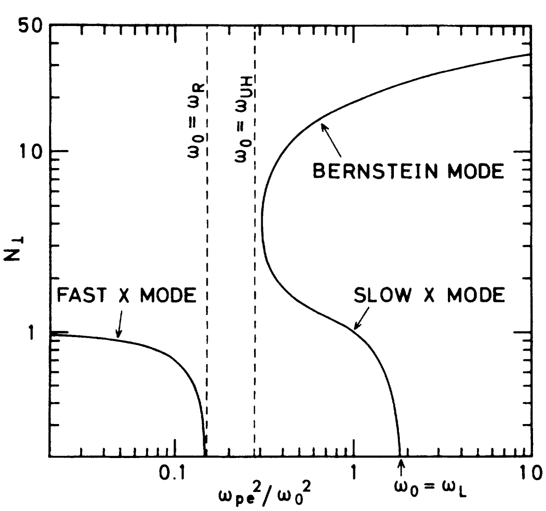

FIG. 1. Refractive index $N_\perp$ vs ω_{pe}^2/ω_0^2 for $\Omega_e/\omega_0=0.85$ and $T_e=1.3$ keV.

First, we will explain the mode-conversion process of a narrow beam of the fast X mode injected obliquely to a static magnetic field. The fast X mode incident from outside the plasma tunnels through the evanescent region between the cutoff ($\omega_0=\omega_R$) and the UHR, and is converted into two modes: one is the Bernstein mode (the FX-B process[4-9]) and the other is the slow X mode. When the plasma density is high enough and the cutoff of the slow mode ($\omega_0=\omega_L$) exists in the plasma, the slow X mode is reflected at the cutoff ($\omega_0=\omega_L$) and is partly converted into the fast mode by the tunnel effect, but is also expected to be partly converted into the B mode at UHR. The last process is the FX-SX-B process. In this case, the conversion points of the fast and the slow X modes into the B modes are different and the two mode-conversion processes can be decomposed and considered to be two independent processes.

Next, in the case of normal injection which we deal with in the particle simulation, an analysis similar to the case of the oblique injection holds. However, the reflected slow X mode propagates along the same trajectory in the opposite direction and is converted into the B mode at the same position where the fast X mode is directly converted into the B mode. In this case, the two processes, the FX-B and the FX-SX-B processes interfere with each other and cannot be decomposed, unlike the oblique injection of the narrow beam.

In order to study the mode-conversion process of ECRW, a $2\frac{1}{2}$-dimensional relativistic electromagnetic particle simulation code PS2M (Ref. 10) is improved and revised by adopting a Courant-condition-free scheme even for the system where the electromagnetic wave of the longest wavelength coexists with the electrostatic waves, whose wavelength becomes very short in the overdensity region. The numerical properties of this Courant-condition-free scheme will be discussed elsewhere.

A schematic diagram of the simulation model is shown in Fig. 2. The system is intended to be representative of a toroidal system with minor radius a in the most simplified way. It is periodic in the y direction and is bounded by a pair of the conducting walls in the x direction. The static magnetic field ($\mathbf{B}_0 \| \mathbf{y}$) is assumed to vary linearly in x and uniformly in y. The external current for generating the fast X mode is located in the vacuum region of the low-field side. The fast X mode propagates in a plasma normally to the static magnetic field. An absorbing boundary condition is imposed on the electromagnetic field at the left boundary and is achieved by the use of a ramp function.[11] The initial profile of electron density is parabolic in the x direction and uniform in the y direction. The maximum density is $3.00n_0$ and $1.55n_L$, where n_0 and n_L are the cutoff densities of the O mode and of the slow X mode, respectively. The initial electron temperature is $T_e = 1.3$ keV. The ions are assumed to be immobile. In order to show the dependence on the density gradient of the mode-conversion process, we have varied the size of the plasma, i.e., the minor radius a, keeping the wavelength of the incident wave in vacuum a constant value λ_0.

The fast X mode is observed to propagate up to the cutoff ($\omega_0 = \omega_R$), as shown in Fig. 3, and to be converted into the B mode at UHR, as shown in Figs. 4(a)-4(c). The slow X mode is also observed to be converted from the fast X mode (Fig. 3) and to be reflected at the cutoff ($\omega_0 = \omega_L$). The reflected slow X mode is expected to be partly converted into a B mode. The observation of this slow X mode suggests the existence of the new mode-conversion process, the FX-SX-B process. The B mode propagates with little damping from UHR to the point just before the electron cyclotron resonance (ECR), and it damps strongly at ECR. In accordance with this wave damping, the electron kinetic energy increases near ECR, where the density is $\omega_{pe}^2/\omega_0^2 = 2.7-2.9$.

As the results in Ref. 12, the energy deposition profile is broad as shown in Fig. 4(a). We believe that this is due to collisional effects or nonlinear effects such as stochastic acceleration. We have carried out preliminary runs with larger wave amplitude or larger likelihood of plasma collision (we used a smaller number of particles than the runs presented in this paper, keeping the plasma density constant). In these runs, we observed a broader energy deposition profile than the result presented, which shows the most peaked energy deposition profile near ECR. In the present runs, however, the number of the particles is not large enough or the wave amplitude is not small enough to eliminate the collisional effects or the nonlinear effects completely.

We believe that the increase of electron kinetic energy near UHR seen in Figs. 4(b) and 4(c) is due to the nonlinear acceleration caused by the larger wave amplitude at UHR than elsewhere. The energy increase beyond the ECR may be attributed to the anomalous diffusion of the perpendicular kinetic energy.

The conversion efficiency from the fast X mode to the B mode can be compared with the absorption coefficient $A = 1 - R$, where R is the reflection coefficient of the incident electromagnetic wave. The reflection coefficient R is measured by separating the electromagnetic wave into an incident wave and a reflected wave in the vacuum region between the antenna and the plasma surface.[12] In Fig. 5, the absorption coefficients A are plotted as a function of $\eta = k_0 \Delta x$, where k_0 is the wave number of the incident wave in vacuum, $2\pi/\lambda_0$, and Δx is a distance be-

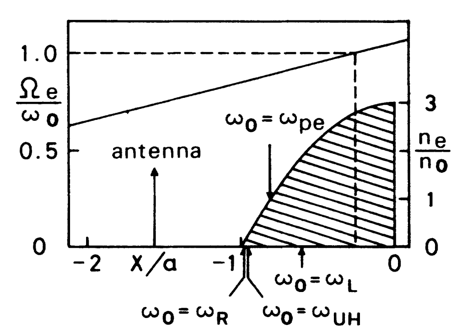

FIG. 2. The normalized electron cyclotron frequency Ω_e/ω_0 and the spatial profile of the normalized plasma density n_e/n_0 vs x, where n_e and n_0 are the electron density and the cutoff density of the ordinary mode, respectively.

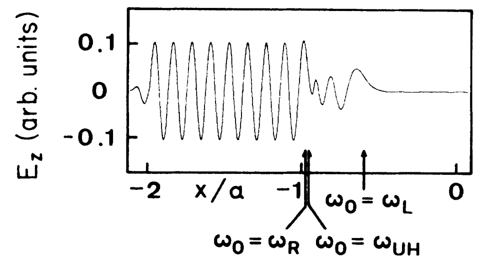

FIG. 3. Interferogram of the electromagnetic field E_z at $t = 725(2\pi/\omega_0)$ for $a/\lambda_0 = 8.24$.

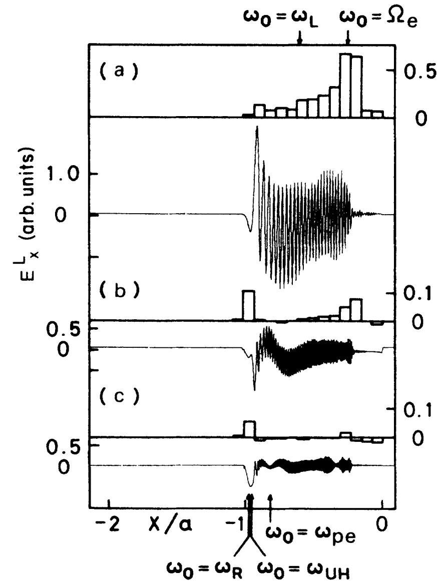

FIG. 4. Interferogram of the electrostatic field E_x^L and the spatial profile of the energy deposition to electrons $\Delta(n_e T_e)/\bar{n}_{e0} T_{e0}$. (a) At $t = 242(2\pi/\omega_0)$ for $a/\lambda_0 = 2.06$; (b) at $t = 483(2\pi/\omega_0)$ for $a/\lambda_0 = 4.12$; (c) at $t = 725(2\pi/\omega_0)$ for $a/\lambda_0 = 8.24$.

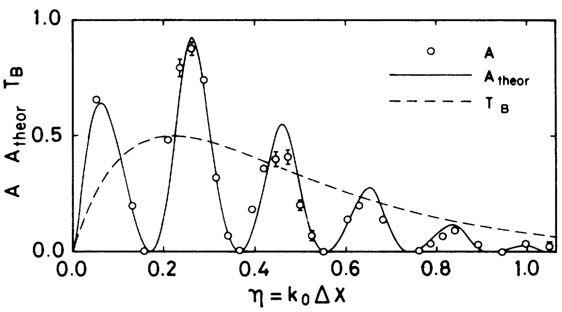

FIG. 5. Absorption coefficients A and A_{theor} and conversion efficiency T_B vs $\eta = k_0\Delta x$. The solid line and the circles indicate the absorption coefficients, A_{theor} and $A = 1-R$, of an incident fast extraordinary mode, where A_{theor} is obtained analytically and $A = 1-R$ is measured in the simulation. The dashed line indicates the mode conversion efficiency T_B from a fast extraordinary mode to a Bernstein mode, where T_B is obtained by combining the Budden's calculations.

tween the cutoff ($\omega_0 = \omega_R$) and UHR. This parameter η is proportional to $n/(dn/dx)$.

The absorption coefficient can be obtained analytically, using some approximations. One approximation is the cold-plasma approximation and the other approximations are those for the electron density profile and the refractive index.

In the cold-plasma approximation, the B modes are ignored and the energy of the B modes is assumed to be absorbed at UHR (this absorption is called the resonance absorption[6]). Therefore, the FX-RA and the FX-SX-RA processes (RA means the resonance absorption at UHR) can be substituted for the FX-B and the FX-SX-B processes, respectively. In other words, the warm-plasma theory of UHR interprets this resonance absorption as conversion into the B modes.[7]

At first, we will show the analytical calculation of the absorption coefficient for the normal injection including the effect of the interference between the FX-RA and the FX-SX-RA processes. The equation for the electric field of the X mode, E_z, is given by

$$\frac{d^2}{dx^2}E_z + k_0^2 N_\perp^2(x) E_z = 0\,, \tag{1}$$

where $N_\perp$ is the refractive index of the X mode. In the cold-plasma approximation, $N_\perp$ is expressed as follows:

$$N_\perp^2(x) = \frac{[1-X(x)+Y(x)][1-X(x)-Y(x)]}{1-X(x)-Y^2(x)}\,, \tag{2}$$

where $X(x) = \omega_{pe}^2(x)/\omega_0^2$ and $Y(x) = \Omega_e(x)/\omega_0$. We divided the system into four regions I–IV. In region II, where the X mode propagates as a fast X mode, reaches the cutoff ($\omega_0 = \omega_R$), and is mode converted to a slow X mode at UHR, the wave equation (1) reduces to Whittaker's differential equation[4] and its solution is represented by Whittaker's functions $M_{k,1/2}$ and $W_{k,1/2}$ when the electron density is assumed to vary linearly and the simplified refractive index[5] is used in this region. In region IV, where the cutoff ($\omega_0 = \omega_L$) is included, the wave equation (1) can approximately be reduced to the Stokes differential equation,[4] when the squared refractive index $N_\perp^2$ is assumed to vary linearly. This solution is expressed by the Airy function A_i. Since there do not exist any zero and singular points of the squared refractive index $N_\perp^2$, we use two independent Wentzel-Kramers-Brillouin solutions in region III. In the vacuum region (region I), the incident and the reflected waves can be expressed by $E_i\exp(ik_0x)$ and $E_r\exp(-ik_0x)$, respectively. When E_i is given, E_r and the other coefficients of the solutions are obtained using the continuity conditions of the electric field of the X mode. The absorption coefficient A_{theor} is given by $A_{\text{theor}} = 1 - |E_r/E_i|^2$, which is indicated by the solid line in Fig. 5. The minimum values which are close to zero, appear periodically for η, and the maximum of the absorption coefficient exists around $\eta = 0.26$ ($a/\lambda_0 = 2.06$) as shown in Fig. 5. The measurements in the simulation have verified these η dependences, and their values agree quite well with the theoretical ones of the absorption coefficient.

The existence of the minimum values which are close to zero in the absorption coefficient can be explained by the interference between the FX-RA and the FX-SX-RA processes; in other words, the interference between the right-propagating slow X mode converted from the fast X mode and the left-propagating slow X mode perfectly reflected at the cutoff ($\omega_0 = \omega_L$): The absorbed energy of the resonance absorption is proportional to $|E_z|^2$ at UHR.[6] Since the position of the resonance absorption in FX-SX-RA process is the same as that of the FX-RA process in the case of normal injection, the total absorbed energy of the resonance absorption is proportional to $|E_z^+ + E_z^-|^2$, where E_z^+ and E_z^- are the complex amplitude of the right- and the left-propagating slow X modes, respectively. Considering $|E_z^+| = |E_z^-|$ at UHR, $|E_z^+ + E_z^-|^2$ becomes zero at UHR when the phase difference between the right- and the left-propagating slow X modes is equal to $(2n+1)\pi$ at UHR, where n is an integer. This means that the FX-RA and the FX-SX-RA processes interfere with each other: When the phase difference is equal to $(2n+1)\pi$, the two processes cancel each other and total absorbed energy becomes zero.

If the interference between the slow X modes can be avoided (for instance, if the narrow beam of the X mode is obliquely injected), the FX-B and the FX-SX-B processes can be assumed to be independent and to be decomposed. Then the total conversion efficiency to the B mode can be evaluated as follows. According to Budden's theory,[4] the transmission coefficient from the fast mode to the slow mode is $T_{FS} = \exp(-\pi\eta)$, and the reflection coefficient of the fast mode is $R_F = [1-\exp(-\pi\eta)]^2$. Combining these results, the conversion efficiency of the FX-B process is calculated to be

$$T_{FB} = 1 - T_{FS} - R_F = \exp(-\pi\eta)[1-\exp(-\pi\eta)]\,.$$

The conversion efficiency from the slow mode to the B mode is $T_{SB} = 1 - \exp(-\pi\eta)$. Therefore, the conversion efficiency of the FX-SX-B process is calculated as

$$T_{FSB} = T_{FS}T_{SB} = \exp(-\pi\eta)[1-\exp(-\pi\eta)]\,,$$

and the total conversion efficiency is

$$T_B = T_{FB} + T_{FSB} = 2\exp(-\pi\eta)[1-\exp(-\pi\eta)]\,,$$

which is plotted as the dashed line in Fig. 5. However, note that this analysis becomes invalid for normal injection, because the interference between the slow X modes is not considered in this simple analysis.

For efficient conversion of the fast X mode to the B mode, the plasma must be small ($a/\lambda_0 \sim 2$) or a steep density gradient is required for large plasmas, when the normalized cyclotron frequency at the plasma surface is $Y=0.85$, which is adopted in the present simulation. When Y is closer to unity at the plasma surface (or top injection is adopted), the evanescent region between the cutoff ($\omega_0=\omega_R$) and UHR becomes smaller. From the analytical calculation, it is found that when Y is 0.95 the optimum density gradient is achieved for $a/\lambda_0=3.21$ and the absorption coefficient $A_{\rm theor}$ is still large ($A_{\rm theor}=0.57$) for a larger plasma ($a/\lambda_0=8.73$).

In conclusion, a new mode-conversion process, the FX-SX-*B* process has been found in high-density plasmas which include the cutoff of the slow X mode. Since the B mode has no density cutoff, this mechanism should be beneficial for heating highly overdense plasmas.

The authors wish to express their gratitude to Dr. R. Sugihara and Dr. A. Fukuyama for useful discussions. This work was partially supported by the Grant-in-Aid for Scientific Research of the Ministry of Education, Science, and Culture in Japan and has been carried out under the Collaborating Research Program at the Institute of Plasma Physics, Nagoya University.

[1]J. Preinhaelter and V. Kopecký, J. Plasma Phys. **10**, 1 (1973); J. Preinhaelter, Czech. J. Phys. B **25**, 39 (1975).

[2]T. Maekawa, S. Tanaka, Y. Terumichi, and Y. Hamada, Phys. Rev. Lett. **40**, 1379 (1978); J. Phys. Soc. Jpn. **48**, 247 (1980).

[3]E. Mjølhus, J. Plasma Phys. **31**, 7 (1984).

[4]K. G. Budden, *Radio Waves in the Ionosphere* (Cambridge Univ. Press, London, 1961), Chaps. 15 and 21.

[5]R. Sugihara, J. Phys. Soc. Jpn. **21**, 786 (1966).

[6]R. B. White and F. F. Chen, Plasma Phys. **16**, 565 (1974).

[7]H. H. Kuehl, Phys. Rev. **154**, 124 (1967).

[8]Merit Shoucri and H. H. Kuehl, Phys. Fluids **24**, 1395 (1981).

[9]H. Sugai, Phys. Rev. Lett. **47**, 1899 (1981).

[10]H. Abe and S. Nakajima, J. Phys. Soc. Jpn. **56**, 3899 (1987). The work presented in this paper can be done by using a one-dimensional code, but we have substituted the two-dimensional code PS2M for it.

[11]P. C. Liewer, A. T. Lin, J. M. Dawson, and M. Z. Caponi, Phys. Fluids **24**, 1364 (1981).

[12]B. L. Smith, H. Okuda, and H. Abe, Phys. Fluids **28**, 1772 (1985).